Two-fold Strategy towards Sustainable Renewable Energy Networks when Uncertainty is Certain

Ankita Garg*, Amritpal Singh†, Gagangeet Singh Aujla*, Hongjian Sun†
*Department of Computer Science, Durham University, Durham, United Kingdom
†Department of Engineering, Durham University, Durham, United Kingdom
E-mail: {ankita.garg, amritpal.singh, gagangeet.s.aujla, hongjian.sun}@durham.ac.uk

***Abstract*—With renewable energy sources (RESs) integrated into modern power systems, energy consumers participate in the energy market making the entire network more complex and uncertain. Therefore, adaptive strategies are needed to address the various uncertainties associated with the energy network to maintain reliability and achieve sustainability. In this research paper, we propose an integrated two-fold approach that combines competitive market mechanisms with cooperative strategies to enhance reliability and resilience in distribution networks under uncertainty. In the normal operational stage, we adopt a competitive approach wherein an optimal price is determined to meet the required consumer demand, facilitating energy sharing among areas and minimising reliance on the grid, thereby reducing carbon emissions associated with conventional energy generation. To detect and identify an uncertain event within the network, a heuristic algorithm is proposed, which determines the hidden inter-dependencies among the different network input parameters. Finally, to mitigate the impact of these identified uncertainties, we introduce a cooperative approach wherein all areas leverage the battery storage facilities to ensure continuity of energy supply and minimise overall losses. During an uncertain event, a maximum reduction of 97% is observed in the carbon footprints for the proposed scheme while maintaining the overall profit.**

***Index Terms*—Bayesian analysis, cooperative strategy, distribution networks, reliability, renewable energy, sustainability**

I. Introduction

With the advent of digitisation and urbanisation, greenhouse gas (GHG) emissions are increasing leading to climate change, impacting the physical environment, and life on this planet. Therefore, there is an urgent need to reduce GHG emissions, control global warming, and alleviate climate change. The energy sector contributes about 34% of the global emissions, wherein the contribution of UK's energy sector is approximately 1% of the global emissions [1]. To achieve the global net-zero emission targets in the energy sector by 2050, there is a need for a transition from fossil fuel to green technologies such as offshore wind, rooftop solar panels, and nuclear power. The global growth in renewable energy capacity has almost doubled in 2023 as compared to 2022 reaching above 500 gigawatts with solar panels alone accounting for one-third of the additions [2]. Distributed energy resources (DERs), such as solar panels, wind turbines, and battery storage systems, enable localised energy generation, reduce transmission losses, and enhance energy security by mitigating dependence on centralised power plants. With the increasing penetration of DERs, the traditional uni-directional power system is becoming bi-directional. The consumers are participating in the energy market by selling and purchasing energy from the power grid, allowing a two-way flow of power [3]. This integration into distribution networks (DNs) offers numerous advantages, including enhanced grid resilience, improved energy efficiency, and increased use of renewable energy sources (RESs), which collectively contribute to reducing carbon emissions and achieving sustainability goals. However, the integration of DERs also presents several challenges and uncertainties. These include technical issues such as maintaining grid stability and reliability amidst intermittent renewable energy outputs [4], ensuring effective communication and control systems for real-time coordination [5], [6], and addressing the complexities of bidirectional power flows [7]. Researchers have employed advanced artificial intelligence methods to predict real-time power generation in the energy networks [8]. However, sometimes there are abnormal events or uncertainties in such networks due to grid congestion, equipment failure, natural disasters, overloading, or other environmental factors. If left unattended, these could lead to cascading failures or outages resulting in power system blackouts or interrupting the reliability of supply [9]. One of the biggest blackouts occurred in Bangladesh in Oct. 2022 due to the 3% rise in the peak energy demand from the forecasted value, which resulted in the grid failure [10].

Motivation Scenario: To analyse the impact of uncertainties associated with the integration of DERs in DNs, we simulated a small residential area with around 100 households in London, UK based on the smart meter energy consumption data[1]. Given the area's climatic conditions, wind turbines were considered as the primary source of renewable energy generation. We synthetically injected an uncertain event where wind generation drops to zero from time t=80 hours to t=90 hours into the system as shown in Fig. 1(a). It can be inferred from Fig. 1(b) that when wind power generation becomes zero,there is an increased dependence on grid purchases to fulfill the load demand (Fig. 1(d)). Since the majority of the power generation from the grid comes from non-renewable sources of energy, the increased grid dependence would increase the corresponding carbon footprints. This case study analysed the impact of

[1]https://data.london.gov.uk/dataset/smartmeter-energy-use-data-in-london-households

uncertainty on carbon emissions for a small residential scenario, and scaling this to a regional or national level further stresses the urgency of the issue [11]. This underscores the critical need to address the challenges posed by such uncertainties to reduce carbon emissions and maintain a reliable power supply. Thus, there is a need to develop robust strategies for detecting and mitigating uncertainties in DER-integrated DNs to ensure the reliability of power supply and simultaneously reduce the dependence on fossil-fuel-generated energy.

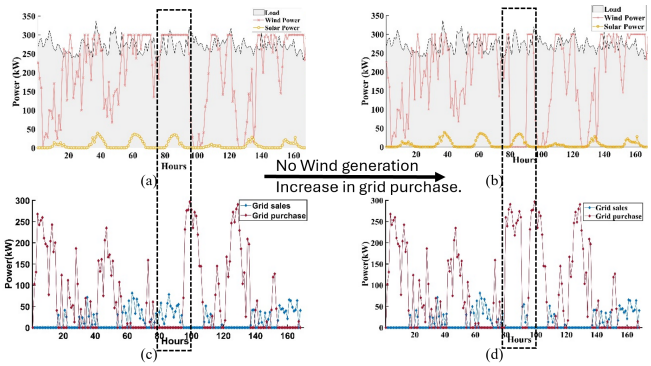

Fig. 1: Increase in grid purchase triggered due to uncertainty in power generation

The traditional deterministic concepts used in power system operation and planning do not consider the uncertainties in DNs due to the inherent variability of RESs, unpredictable consumer demands, and data quality issues [12]. These models cannot handle the complexities of DER integration, regulatory changes, and cybersecurity risks [6], [13]. The existing stochastic methods such as probabilistic approaches, possibilistic approaches, hybrid approaches, information gap decision theory, and robust optimisation, have been well explored in the literature [14]–[16]. The main purpose of these methods was to measure the impact of uncertain input parameters on the system output parameters based on historical data. However, prior knowledge of an uncertain input's pre-defined probability distribution function is required in these methods. To overcome this limitation, a data-driven two-stage stochastic optimisation algorithm was proposed in [17] to model the uncertainty in DN output parameters. In this article, the authors used the decomposition method for the parallel computation of uncertain parameters to reduce the dependence on prior knowledge for both stages. An optimisation algorithm based on the concept of Conditional Value at Risk that models the uncertainty in demand and energy prices was proposed in [18] to enhance renewable energy generation while minimising operational costs. All these methods have considered no correlation among the different uncertain parameters, which is not feasible in a complex power system network, where parameters are correlated to each other. Therefore, there is a need to identify the hidden inter-dependencies among the hidden uncertain parameters in the network, which can be done using the Bayesian network approach. The authors in [19] proposed a physics-informed probabilistic graph convolution network to predict the voltages within the DNs integrated with solar panels and electric vehicles. The authors used the Bayesian interface to quantify the uncertainty in the network topology at the planning stage. Despite the accurate predictions, real-time (or operational) uncertainties can impact the power system operation. So, further research is required to uncover the potential of addressing these uncertainties. The Bayesian network's ability to model complex inter-dependencies and update beliefs based on new data makes it advantageous for real-time uncertainty detection and management. In [20], an optimal strategy for mitigating voltage imbalances in DERs was proposed through the joint allocation of energy storage systems. This approach aimed to stabilise voltage profiles by strategically deploying storage devices. Similarly, [21] explored a mitigation strategy designed to address congestion in multi-operator flexible market systems for energy trading. However, both studies did not address the impact of uncertainty on carbon emissions associated with these systems. The potential for reducing carbon footprints through these uncertainty mitigation strategies remains unexplored.

Addressing the above mentioned issues, our research proposes a two-fold strategy to mitigate the impact of uncertainties in the DNs. This two-fold approach employs the concept of competition and cooperation among the neighbouring areas before, during, and after the uncertain event. The entire system is segmented into distinct stages, as shown in Fig. 2: data collection, energy modeling, uncertainty detection, and mitigation.

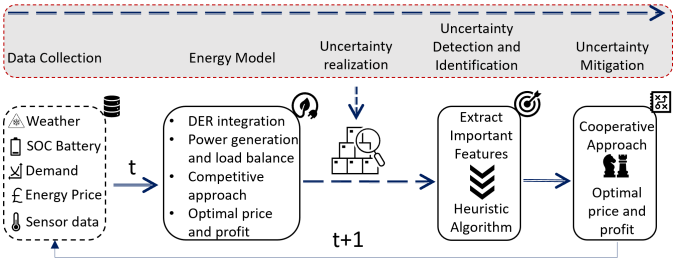

Fig. 2: Research overview

The DERs are integrated into the energy model to compute the total power generation and load balance in the network at time t. Upon realising an uncertain event, a heuristic algorithm is employed to identify its type. (Our preliminary work for uncertainty identification has been presented in [22].) This information is then processed by a cooperative algorithm designed to mitigate the impact of the identified uncertainty on the system. A detailed description of the work carried out in these stages is given in Section III. Considering the real-time problem described above, the major contributions of this research are as follows.

- We propose carbon-aware optimization strategy for the energy network, utilising a competitive approach to determine optimal pricing during normal operations to minimise carbon emissions across the distribution network.
- We propose an algorithm to detect and identify uncertain events within the energy network by establishing hid-

den dependencies among the uncertain parameters using Bayesian networks which is further used to mitigate the impact of uncertainty.
- We propose a novel cooperative strategy for the localised areas mitigating the impacts of uncertainty by preventing the escalation of local problems into entire network disruptions, ensuring stable and reliable energy distribution.

The rest of the paper is organised as follows. Section II illustrates the considered system model for DN integrated with DERs. Section III discusses the proposed methods in detail, while the results are highlighted in Section IV. The paper is finally concluded in Section V.

II. System Model

Fig. 3 illustrates the structure of the power system enabling a two-way flow of power, featuring a power generating sources transmitting energy through the transmission network to the DN as well as allowing consumers to both sell excess energy back to the grid and purchase energy when needed. Within the DN, DERs are integrated and connected to consumers, facilitating decentralised energy generation and consumption (modeled as per IEEE Std 1547-2018 [23]). Distribution system operators (DSOs) are responsible for ensuring a reliable power system from the transmission network to the consumers. In this study, as illustrated in Fig. 3, we consider two types of DSOs: the regional DSO (DSO-RC) and the global DSO (DSO-GC). The DSO-RC is responsible for managing energy requests from the local communities (LCs) and maintaining power reliability within small regional areas (A). The DSO-GC, on the other hand, oversees the overall management, operation, and control of the entire DN, handling all incoming and outgoing requests from the DSO-RC to ensure seamless network operations. The

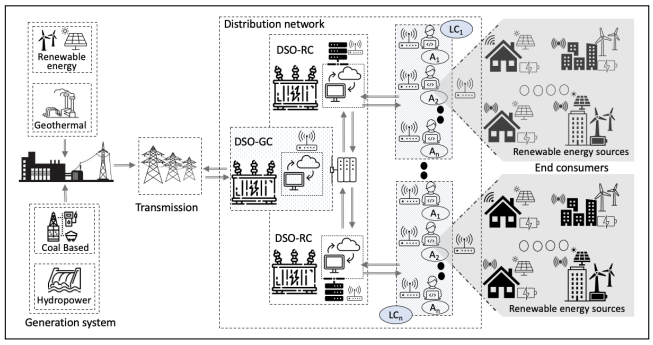

Fig. 3: System model with DERs integrated DN

total renewable energy generation $P^i_{GR}(t)$ at any time t in i^{th} area can be calculated as:

$$P^i_{GR}(t) = P^i_{pv}(t) + P^i_w(t) \tag{1}$$

where $P^i_{pv}(t)$ and $P^i_w(t)$ are the solar and wind power generations of i^{th} area at time t.

The solar power $P^i_{pv}(t)$ generated by each solar panel within an area at time t is calculated using Eq. (2) [24],

$$P^i_{pv}(t) = N^i_{pv} P_{peak} D_{pv} \left[\frac{G^i_T(t)}{G_{STC}}\right] [1 - \tau_p(T^i_C(t) - T_{C,STC})] \tag{2}$$

where P_{peak} represents the peak output power of the PV module, D_{pv} denotes the derating factor, τ_p is the power temperature coefficient, $G^i_T(t)$ and G_{STC} represent incident solar radiance on the PV module at time t and under standard testing conditions, respectively. Additionally, $T^i_C(t)$ stands for the PV panel temperature at time t, $T_{C,STC}$ represents PV cell temperature under standard testing conditions, and N^i_{pv} represents the total number of panels connected in series and parallel. The optimal location, capacity, and number of DERs in a particular area have been calculated beforehand using multi-integer linear programming [25].

Similarly, the real-time wind power, P^i_w, generated by each wind turbine within i^{th} area at time t is expressed by [26]:

$$P^i_w(t) = \begin{cases} 0, & v^i(t) \le v_{ci} \text{ or } v^i(t) \ge v_{co} \\ N^i_w P^r_w(\frac{v^i(t) - v_{ci}}{v_r - v_{ci}}), & v_{ci} \le v^i(t) \le v_r \\ N^i_w P^r_w, & v_r \le v^i(t) \le v_{co} \end{cases} \tag{3}$$

where $v^i(t)$ denotes wind speed at time t, v_{ci} and v_{co} represent the cut-in and cut-off wind speeds, respectively, v_r represents rated wind speed, P^r_w is the rated wind turbine power, and N^i_w depicts the number of wind turbines installed in i^{th} area.

The battery energy storage system (BESS) plays an important role in managing the consumer energy demand when the power generated from the DERs is not sufficient. The charging and discharging of the battery power for i^{th} area, P^i_b, can be calculated as [27]:

$$P^i_b(t) = P^i_b(t-1) - \begin{cases} \eta_{ch}(P^i_{load}(t) - \frac{P^i_{GR}(t)}{\eta_c}) \text{ ; charging} \\ \eta_{dch}(\frac{P^i_{load}(t)}{\eta_c} - P^i_{GR}(t)) \text{ ; discharging} \end{cases} \tag{4}$$

where P^i_{load} is the load demand of i^{th} area, η_c is the converter efficiency, η_{ch} and η_{dch} are the battery charging and discharging efficiencies, respectively.

The operational strategy used to simulate each area's energy system dynamics is indicated in Algorithm 1. The expected power generation, $P^{exp}_{GR}(t)$, for each area and at time interval t is calculated using the Eq. (1) and is compared with its real-time value, $P^{rt}_{GR}(t)$. If these values match, then a carbon-aware energy scheduling algorithm is run, that manages the load demand of an area by using renewable energy generation or charging/discharging the battery. The excess generation from the neighboring area is sold to the deficient areas based on the price calculated using the competitive game model described in Section III-A. If the real-time and expected values do not match, then an uncertainty detection and identification algorithm (Algorithm 2) is triggered as described in Section III-B. If there is an uncertainty present in the system, then it is mitigated using the uncertainty mitigation algorithm (Algorithm 3) detailed in Section III-C.

Algorithm 1: Distribution Network System Operation

Input: **Area Request:** $i \in A, i = 1, 2, \ldots, n$
Output: Profit, π
while *($i \neq NULL$)* **do**
  Compute: P_{GR}^{exp}, P_{GR}^{rt};
  if *($P_{GR}^{exp} \simeq P_{GR}^{rt}$)* **then**
    Execute: *Carbon-aware energy scheduling*;
    if *($P_{GR}^{i}(t) > P_{load}^{i}(t)$)* **then**
      if *($SOC^{i}(t) < SOC_{max}(t)$)* **then**
        Alert: $\rightarrow$ *CHARGE BATTERY*;
      end
      else
        Sell Energy $\rightarrow$ **Competitive Theory Approach** ▷ Section: III-A;
      end
    end
    else
      if *($SOC^{i}(t) > SOC_{min}^{i}$)* **then**
        Battery Status (D) $\rightarrow$ *DISCHARGED*;
      end
      else
        Use Competitive Theory Approach ▷ Section: III-A
      end
    end
  end
  else
    Call Function: $\rightarrow F =$ UDI(i) ▷ Algorithm: Alg. 2;
    if *($F == A_\delta$)* **then**
      Call Function: $\rightarrow P =$ UM(i) ▷ Algorithm: Alg. 3
    end
    Update: $P_G^{exp} = P$ & **Go to Step 3** ▷ Check the condition
  end
end

The DN system model described in this section highlights the fundamental principles and equations governing energy distribution and generation within the network. To enhance the robustness and reliability of the DN, we propose a novel scheme that incorporates state transitions to manage the network's response to different phases of operation: healthy, fractured, and recovered. This proposed scheme is illustrated through a state transition diagram and detailed in the following section.

III. Proposed Scheme

The proposed scheme focuses on the DN's operation into three distinct phases as shown in Fig. 4. These are 1) Healthy (or Normal) Phase, 2) Fractured (or Uncertain) Phase, and 3) Recovered (or Mitigation) Phase. These phases are based on the behaviour of the system before and after the occurrence of uncertain events, providing a comprehensive framework for understanding and addressing system disruptions. The control

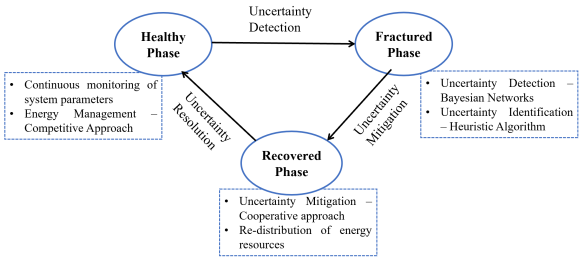

Fig. 4: Phase transition diagram

actions for the three phases leverage three novel approaches designed to ensure the reliability of the DN. These approaches not only maintain the network's reliability but also optimise regional profitability and minimise carbon emissions. In the healthy phase, the system operates under optimal conditions with efficient energy management and minimal carbon footprint. During the uncertain phase, an advanced Bayesian algorithm is employed to detect and mitigate the impacts of uncertainties, such as fluctuating renewable energy output or unexpected load variations. Finally, in the recovery phase, the system employs robust strategies to restore normal operations while continuing to optimise economic and environmental outcomes. A detailed description of the proposed approaches used in the three phases is as follows.

A. Healthy / Normal Phase

This phase signifies the desired and stable operational mode, where the power system is capable of meeting the consumer load demand. During normal operation of the DNs, a competitive energy-based demand-supply model is employed to determine the optimal energy price offered by each area and their corresponding profits. By leveraging competitive dynamics within the areas, this model seeks to minimise reliance on the grid, thus reducing grid purchases and subsequently decreasing the overall carbon footprints.

The market price of the energy depends on the demand for the energy in the market, and to compute its optimal value, a linear relationship is established between the demand (D) [28] and supply of the energy available in the market as given below.

$$D = B - e \cdot p \tag{5}$$

where p is the optimal market price of the energy, D is the total demand, e is the elasticity coefficient, and B is the intercept. To maintain the balance between total energy and demand, all the areas must fulfill the energy demand. Suppose there are n areas supplying the energy, D must be fulfilled by the total quantity Q of energy produced by the area as mentioned below:

$$D = \sum_{i=0}^{i=n} Q_i \tag{6}$$

During production of the energy by i^{th} area ($i = 1, 2, ..., n$), there is also a marginal cost, C_i, incurred to generate Q_i quantity of energy which is calculated by:

$$C_i = \alpha_i \cdot Q_i^2 + \beta_i \cdot Q_i + \gamma_i \tag{7}$$

where α_i and β_i are marginal cost coefficients for i^{th} area corresponding to thermal power generation, γ_i represents fixed costs or capital costs associated with renewable energy installations that are not directly proportional to the quantity of energy generated Q_i. We utilised the Cournot Game model to simulate and analyse the energy transactions among suppliers. This model effectively represents and understands the dynamics of competing markets in this context [28].

1) Cournout Game Model: The main aim of an area participating in the energy ecosystem is to maximise its profit. The profit of i^{th} area (π_i) is calculated by the price quoted by an area in the market minus the marginal cost of the energy production as mentioned below:

$$\max_{(Q_i, i=1,2,\ldots,n)} \pi_i = p \cdot Q_i - C_i \cdot Q_i \tag{8}$$

$$s.t. \sum_{i=0}^{i=n} Q_i = B - e \cdot p \tag{9}$$

$$Q_i^{min} < Q_i < Q_i^{max} \tag{10}$$

where Q_i^{min}, Q_i^{max} are the minimum and maximum production of energy by the i^{th} area. The price p is calculated by using Eq. (9) as mentioned below:

$$p = \frac{B - \sum_{i=0}^{i=n} Q_i}{e} \tag{11}$$

The profit of i^{th} area is calculated by adding its revenue from the game model to the income from any contracts and then subtracting its generation costs. So, we redefine the optimization problem for calculating the profit as follows:

$$\max_{(Q_i, i=1,2,\ldots,n)} \pi = p \cdot (Q_i - C_i) - C_i \cdot Q_i \tag{12}$$

Formulating the Eq. (12) by substituting the value of p from Eq. (11) gives:

$$\max_{(Q_i, i=1,2,\ldots,n)} \pi = \frac{B - \sum_{i=0}^{i=n} Q_i}{e} \cdot (Q_i - C_i) - C_i \cdot Q_i \tag{13}$$

The price equilibrium is obtained by using the Kuhn-Karesh-Tucker (KKT) condition [29] highlighted below:

$$\frac{\partial \pi_i}{\partial Q_1} = \frac{B - \sum_{i=0}^{i=n} Q_i}{e} - \frac{Q_i - C_i}{e} - C_i + \phi_i^{min} - \phi_i^{max} = 0 \tag{14}$$

where ϕ_i is the Lagrange multipliers associated with the inequality constraints. Substituting $\frac{B - \sum_{i=0}^{i=n} Q_i}{e}$ by p using Eq. (11), gives:

$$\frac{\partial \pi_i}{\partial Q_1} = p - \frac{Q_i - C_i}{e} - C_i + \phi_i^{min} - \phi_i^{max} = 0 \tag{15}$$

$$\phi^{min} \geq 0, (Q_i - Q_i^{min}) \geq 0, \phi_i^{min}(Q_i - Q_i^{min}) = 0 \tag{16}$$

$$\phi^{max} \geq 0, (Q_i^{max} - Q_i) \geq 0, \phi_i^{max}(Q_i^{max} - Q_i) = 0 \tag{17}$$

2) Nash Equilibrium Solution: In this model, the areas ($A_1, A_2, \ldots, \mathrm{A}_n$) submit their offers simultaneously to the RC to participate in the competition model. In this model, there is no cooperation among the participating areas. The utility/profit function is calculated based on the defined inequality constraints. In the defined model, the inequality constraints are defined to maximise the profit of the area and the energy consumer. The defined model works statically due to the non-cooperative behaviour of the participating areas. Due to the static model, the game is defined to maximise the profits of the areas, denoted as (A, π) and elaborated below:

- $A = \{A_1, A_2, \ldots, A_n\}$ are the areas participating in the defined model.
- $\pi = \{\pi_1, \pi_2, \ldots, \pi_n\}$ are the set of utility functions calculated to maximise the profit of the participating areas.

In this game, the areas have to calculate the profits concerning the value of Q. Considering the scenario of two areas, the utility function is calculated as below:

- In the utility matrix, π_1 and π_2 represent the profit of the A_1 and A_2 for a given combination of Q_1 and Q_2.
- The inequality constraints ϕ_{min} and ϕ_{max} are calculated using Langrange multipliers as mentioned below:

$$\phi_{min} = \frac{\mu}{C_1} \tag{18}$$

$$\phi_{max} = \frac{\mu}{C_2} \tag{19}$$

  where, μ is the complementary slackness condition, and C_1, C_2 are the costs of the respective areas.
- The $\pi_{i/j}^{A}$ represents the profit function for i^{th}/j^{th} area corresponding to $A \in \{A_i, A_j\}$ with respect to the Q.

To reach the Nash Equilibrium, the utility matrix to access the possible behaviours of the areas is depicted in Table I.

TABLE I: The Utility Matrix of i^{th} area considering j^{th} area

Area A_i		
	Q_j = min	Q_j = max
Q_i = min	$\pi_i^{(A_i,A_j)}$	$\pi_i^{(A_i,A_j)}$
Q_i = max	$\pi_i^{(A_i,A_j)}$	$\pi_i^{(A_i,A_j)}$

B. Fractured / Uncertain Phase

This phase occurs when there is an uncertainty or abnormality observed within the system. In coordination with the competitive energy sharing model described in Section III-A, we employ a Bayesian network (BN) approach [22] to effectively detect uncertain events within the distribution system. The BN is utilised to find the conditional probabilities among the uncertain variables computed using the complex Bayesian algorithm. It is a form of semi-naive Bayesian Learning that introduces a complex structure to capture inter-dependencies among variables, thereby alleviating the assumption of attribute independence made by the Bayes approach. Once an uncertain event is detected, an heuristic algorithm (described in Algorithm 2), as proposed in [22], is utilised for identifying the type of uncertainty. By combining the power of Bayesian inference with the heuristic algorithm, our approach ensures accurate and timely identification of critical events, thereby enabling proactive responses to mitigate their impact.

If the power generation values align with expectations, the LC proceeds with normal operations. However, if inconsistencies arise, the LC employs a Bayesian analysis to determine the probability distribution of G or v, and find their respective ranges (G_{min}, G_{max}) or (v_{min}, v_{max}). Based on these, using the Eq. (2) and Eq. (3), the range of solar $(P_{PV}^{min}, P_{PV}^{max})$ and wind power $(P_{w}^{min}, P_{PV}^{w})$ generation can be calculated. If the

Algorithm 2: Uncertainty Detection and Identification

Input: $G_{min,max}, V_{min,max}$; i: Area Request
Output: A_δ: State of uncertainty in area ▷ δ: Uncertainty

// Define the state of the request
Function UDI (i) **:**
  if $(P_{PV}^{exp}(i) \neq P_{PV}^{rt}(i)$;
  & $P_{PV}^{rt}(i) \notin (P_{PV}^{min}(i), P_{PV}^{max}(i)))$ **then**
    Assign: $A_i \leftarrow A_\delta$;
    ▷ Data Uncertainty
  end
  else if $(P_{w}^{exp}(i) \neq P_{w}^{rt}(i)$;
  & $P_{w}^{rt}(i) \notin (P_{w}^{min}(i), P_{w}^{max}(i)))$ **then**
    Assign: $A_i \leftarrow A_\delta$;
    ▷ Data Uncertainty
  end
  else if $(P_{load}^{exp} \neq P_{load}^{rt})$ **then**
    Assign: $A_i \leftarrow A_\delta$;
    ▷ Behavioural Uncertainty
  end
  else
    Assign: $A_i \leftarrow A_\delta$;
    ▷ Weather Uncertainty
    Send signal: *Normal* $\xrightarrow{ack}$GC ▷ GC: Global Controller
  end
  return A_δ ;
end

real-time values fall outside this range, it indicates potential weather uncertainty. Otherwise, the mismatch may be attributed to faulty data, which could stem from various sources such as faulty or dead sensors (erratic/uniform/zero readings from a sensor) and data manipulation (intentional alteration of data). If none of these, the uncertainty is attributed to the change in consumer behavior by comparing the expected (P_{load}^{exp}) and real-time (P_{load}^{rt}) values of the consumer demand of an area.

C. Recovered / Mitigation Phase

Whenever an uncertain event is identified in an area a, we propose a novel cooperative strategy, to mitigate its adverse effects on the entire DN. This strategy is grounded in the notion that rather than operating in isolation to maximise their individual profit (as in the case of competitive strategy), all areas collaborate to address the issue at hand by pooling resources to support the affected area under uncertainty in minimising overall grid dependency and carbon footprints as described in Algorithm 3.

In Algorithm 3, at each time instant, the total surplus energy of all areas sold to the grid are checked. If this energy is enough to meet the required load demand, then it is sold to the affected area at the optimal price as described in the competitive approach using Eq. (11). If the total energy sold to the grid ($P_s(t)$) is not enough, then the battery of the affected area (f) will be discharged according to the power discharge rate function depicted in Eq. (20) until its state of charge SOC^f is equal to a threshold value (ρ = 30%).

$$P_{dis}^{f}(t) = \frac{\mathrm{d}SOC^{f}(t)}{\mathrm{d}t} = -k \cdot SOC^{f}(t) \tag{20}$$

where k is the battery discharging coefficient.

Algorithm 3: Uncertainty Mitigation

Input: Area Request State: $A_i \leftarrow$ Alg. 2 ,
Set SOC: **Threshold1**$\rightarrow \rho$, **Threshold2**$\rightarrow \sigma$, **Threshold3**$\rightarrow \psi$,
Instance of time: t.
Output: **Power purchased from grid:** $P_grid(t)$

Function UM (i) **:**
  Compute: P_{req}^{f}, P_{GR}^{f};
  if $(P_{req}^{f} \geq P_{GR}^{f}$;
  & $SOC^{f}(t) > \rho)$ **then**
    Discharge Battery $\xrightarrow{till}$ ρ;
  end
  else
    if $(\sum P_{sales}^{i}(t) > 0$) **then**
      if $(P_{sales}^{i}(t) > P_{req}^{f}(t))$ **then**
        Competitive theory approach
      end
      else
        Calculate: $P_{rem}^{f}(t) = P_{req}^{f} - \sum P_{s}^{i}(t)$;
      end
    end
    else
      Assign: $P_{rem}^{f}(t) = P_{req}^{f}$;
      if $(SOC^{f}(t) > \sigma$ **then**
        Compute: E_{dis}^{i}; ▷ using Eq. (25)
      end
      else if $(SOC^{f} > \psi)$ **then**
        Discharge Battery $\xrightarrow{till}$ ψ;
        Compute: E_{dis}^{i}; ▷ using Eq. (25)
      end
      else
        Assign: $P_{rem}^{f}(t) = P_{req}^{f}(t)$;
      end
    end
  end
  $P_{grid} = P_{rem}^{f}(t)$;
  return P_{grid};
end

Integrating the power discharge rate function over time determines the energy discharged using:

$$E_{dis}^{f}(t) = \int_{t_1}^{t} P_{dis}^{f}(t)\,\mathrm{d}t \tag{21}$$

If the battery discharge is not sufficient to meet the load demand of that area, then the neighbouring areas with SOC^i ($i = 1, 2, \ldots, n; i \neq f$) greater than the threshold (σ = 60%) will discharge their batteries to meet the load of the energy-deficient area. The battery discharge of the neighbouring areas can be carried out in three possible ways.

- *Entire energy purchased from one area only:* If the chosen firm has sufficient battery storage, it can ensure uninterrupted energy supply to the affected area such that:

$$E_{\text{dis}}^{i}(t) \geq E_{req}^{f}(t) \tag{22}$$

  where $E_{\text{dis}}^{i}(t)$ is the energy discharged by i^{th} area at time t and $E_{req}^{f}(t)$ is the energy required by faulty (or uncertain) area at time t.
- *Equal energy purchase:* In this case, selected areas would discharge an equal amount of their battery storage to meet the required load demand represented below.

$$E_{\text{dis}}^{i}(t) = \frac{E_{req}^{f}(t)}{n} \tag{23}$$

  where n is the total number of areas selected whose $SOC^i > \sigma$ and $i \neq f$.

- *Proportionate energy sharing:* Proportionate energy sharing ensures that each area contributes based on its available capacity. Areas with greater battery storage contribute more, while those with smaller battery storage contribute proportionately less. The proportion of the required energy demand allocated to area i is depicted by:

$$Prop_i(t) = \frac{E^i_{avl}(t)}{E_{\text{total\_sup}}(t)} \tag{24}$$

where $E_{\text{total\_sup}}$ is the total energy supplied by all areas and is calculated as $\sum_i E_i$, such that $i = 1, 2, \ldots, n; i \neq f$, and E_i be the energy supplied by the i^{th} area. The proportional energy allocated to i^{th} area in this case is given as:

$$E^i_{dis}(t) = Prop_i(t) \cdot E^f_{req}(t) \tag{25}$$

This case ensures fairness in the system and therefore is used as the default strategy in the proposed scheme for battery discharge in neighbouring areas.

If there is no area with $SOC^i > \sigma$, then check the areas with $SOC^i > \psi$, where $\psi \leq \sigma$ (and is set at 50%), and follow the same procedure for battery discharging as mentioned in the Eq. (24) and Eq. (25). The final step involves purchasing the energy from the grid E_{grid}, in case none of the neighbouring areas can meet the load demand of the affected area.

The cooperative strategy is designed such that even during an uncertain event while supporting the affected area to meet its load demand, the supplying areas do not incur any loss. The optimal price at any time t during uncertainty is calculated as:

$$p_r(t) = \begin{cases} p(t), & E_{sales}(t) \geq 0 \\ p^{grid}_r(t), & E_{sales}(t) \leq 0 \text{ or } \eta = 0 \\ p^i_r(t), & \eta \neq 0 \end{cases} \tag{26}$$

where $p(t)$ is the price calculated using Eq. (11), $p^{grid}_r(t)$ is the market price offered by the grid at time instant t, E_{sales} is the total energy sold to the grid ($E_{sales}(t) = \sum E^i_{sales}$; E^i_{sales}) is the energy sales of an individual area), η is the number of selected areas to supply energy and $p^i_r(t)$ is the cooperative price offered by the selected firm to the affected firm which is formulated using:

$$p^i_r(t) = \begin{cases} E^i_{grid}(t+1) \cdot p(t+1), & E^i_{grid}(t+1) \geq 0 \\ \xi \cdot E^i_{dis}(t) \cdot C^i(t), & otherwise \end{cases} \tag{27}$$

where ξ is the profit margin of an area, E^i_{grid} is the energy purchased by an area from the grid. The associated carbon footprints (CF) at any time instant can be calculated using:

$$CF(t) = CI \cdot \sum_{i=1}^{n} E^i_{grid}(t) \tag{28}$$

where CI is the carbon intensity and E^i_{grid} is the energy purchased by i^{th} area from the grid.

IV. Results and Discussion

The primary objective of this study is to analyse the behavior of an energy system in response to uncertain events and develop strategies to mitigate their impact, with a particular emphasis on reducing overall carbon footprints. To achieve this, we have considered nine regions (LCs) within England, each comprising multiple areas (denoted by *A*) as depicted in Fig. 5. One such LC (Newcastle) consisting of ten areas is highlighted in this figure. These areas are further equipped with DERs to meet their respective load demands.

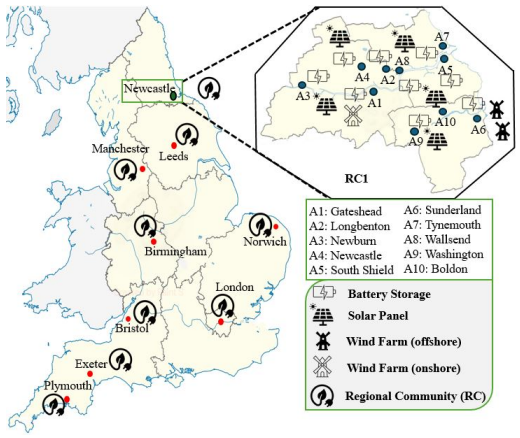

Fig. 5: Considered areas for simulation

In our model, we employ a Regional Controller (RC) at the local level and a Global Controller (GC) at the central level. The RC is responsible for managing incoming and outgoing energy requests within its respective LC, while the GC checks energy scheduling and coordination at the regional level. By focusing on reducing carbon footprints, the study aims to enhance the sustainability of the energy DN under uncertainty. For instance, when an uncertainty such as a sudden drop in renewable generation occurs, the AC would first seek to balance the energy deficit using stored renewable energy within the respective LC or by purchasing surplus renewable energy from neighboring LCs. Only as a last resort would the AC draw energy from the main grid, thereby minimising the carbon impact.

Assumptions: To effectively simulate the system's behavior in handling uncertainties, the proposed study has made the following realistic assumptions.

- The types of uncertainties that can occur in the DN are:
  - *Weather Uncertainty:* It relates to sudden weather changes that deviate from predicted values.
  - *Data Uncertainty:* It depicts faulty sensors or equipment failures that can lead to malicious data being received at the RC.
  - *Behavioral Uncertainty:* It is associated with sudden increases/decreases in load demand at the consumer end.
- During normal operation, the excess generation areas must sell energy to energy-deficient areas before selling it to the grid to minimise the overall carbon footprints.

- During an uncertain event, all the areas in an LC would support the area under uncertainty by selling their excess generation. If there is no excess renewable energy generation in any area, these areas will discharge their batteries to support their neighbouring area under uncertainty.

A. Normal Phase

For normal operation, weather data was systematically collected for one year, spanning from Jan 01, 2023, to Dec 31, 2023 [30], from 10 distinct locations of Newcastle in CSV format. Each location's data after pre-processing (as explained in IV-B) is stored in a dedicated file and has 14 distinct meteorological parameters. The energy price data for energy sales and purchased is gathered from UK's energy provider website [31]. It is assumed that the sensors deployed at each DER yield generation data estimated using Eq. (1) and Eq. (2) for solar and wind resources, respectively. The energy profile of one week for one area in Newcastle (i.e., Gateshead), is shown in Fig. 6. Fig. 6(a) depicts the wind and solar generation in this area as well as its overall load demand. Fig. 6(b) highlights the power purchased from the grid during low renewable energy generation and sold to the grid during high renewable energy generation within the depicted time duration.

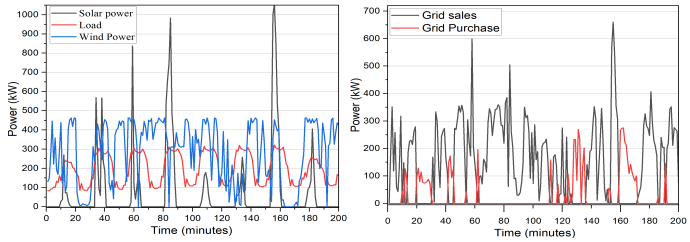

(a) (b)

Fig. 6: Energy profile of an area (a) Power generation and load demand (b) Power sold and purchased from grid

Furthermore, in the normal operational phase, all areas will be participating in the energy market based on their individual renewable energy generation. To better understand the defined competitive game model in Section III-A, we present a case study to calculate the Utility Matrix using collected data points from 10 different areas in the United Kingdom. The utility matrix is calculated using two areas (the Gateshead and Longbenton areas) and the notations for which are defined in Table II.

TABLE II: Notation values in the Case Study

Notation	Value	Description
A_1	Gateshead	First area name
A_2	Longbenton	Second area name
D_{yr}	1	1st day of year data
C_1	0.1595	Cost of A_1
C_2	0.2102	Cost of A_2
Q_1	[0:15819]	Range of produced quantity by A_1
Q_2	[0:69115]	Range of produced quantity by A_2
ϕ_{min}	0	Inequality constraint
ϕ_{max}	0	Inequality constraint

Source: $(C_1, C_2)\leftarrow$ [31], $(Q_1, Q_2, \phi_{min}, \phi_{max})\leftarrow$*Simulation results*

- A_1 initiates the game procedure along with the A_2 and quotes 0.1595 costs per required unit to the consumer.
- In a similar pattern, A_2 quotes 0.2102 cost for the same requirement.
- The ϕ_{min} and ϕ_{max} is calculated as 0 using best response optimisation approach [32]. This could occur if the market price p is always greater than or equal to the total costs $C_1Q_1 + C_2Q_2$, leading to an inactive complementary slackness situation.
- The minimum and maximum range of the A_1 is highlighted as [0:15819] and A_2 as [0:69115] from the collected data points corresponding to Gateshead and Longbenton areas.
- The price p corresponding to both areas is calculated using Eq. (11), and the Utility Function (π) is calculated using Eq. (8).

The Utility Matrix corresponding to both areas is mentioned in the Tables III and IV.

TABLE III: The Utility Matrix of A_1 area

	Area A_1	
	Q_2 = 0	Q_2 = 69115
Q_1 = 0	0	0
Q_1 = 15819	3.9911*e^{07}	3.9911*e^{07}

TABLE IV: The Utility Matrix of A_2 area

	Area A_2	
	Q_2 = 0	Q_2 = 69115
Q_1 = 0	0	-0.0001*e^{08}
Q_1 = 15819	0	1.7437*e^{08}

This intense competition ultimately leads to a market equilibrium, a delicate balance where each area's profit is optimised, and more importantly, the collective energy needs of the seekers (consumers) are effectively fulfilled under normal conditions.

Fig. 7 shows the results based on the competitive approach for the entire region as described in Section III-A and the following inferences can be drawn.

The market price offered by the areas with excess renewable energy generation is shown in Fig. 7(a). The zero price indicates that at that time instant there is no energy demand from the neighbouring areas and hence, no energy would be sold to any area. Fig. 7(b) shows the amount of energy met by the surplus renewable energy in the neighbouring areas using the competitive approach. When there is no surplus energy, the remaining energy demand is met by purchasing from the grid. The comparison of carbon footprints with and without using the competitive approach is highlighted in Fig. 7(c). As the excess generation of neighbouring areas meets the major amount of energy demand, therefore, the proportion of energy purchased from the grid is reduced, resulting in a reduction in carbon emissions by approximately 80%.

B. Uncertainty Detection and Identification

To detect and identify the occurrence of uncertain events, the BN approach as described in Section III-B is utilised.

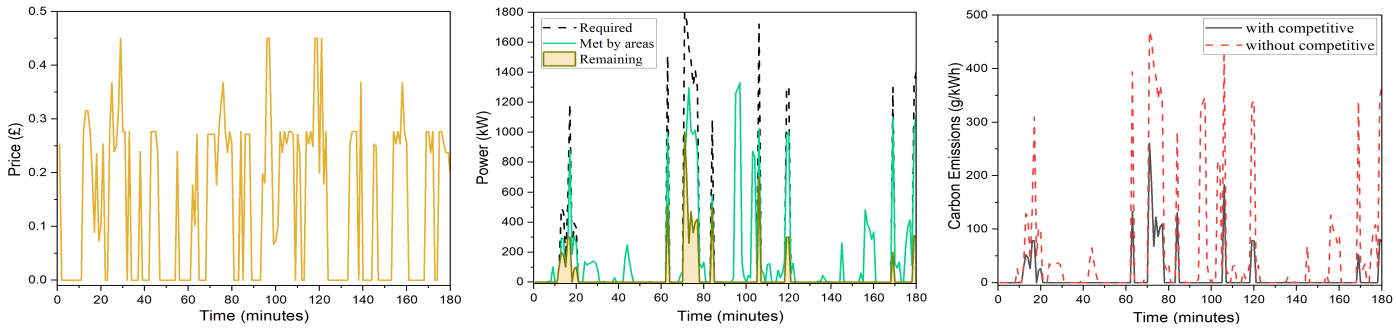

(a) (b) (c)

Fig. 7: Healthy phase results (a) price offered by neighbouring area (b) energy demand met by areas (c) carbon emissions

A structured data discretisation process is implemented by employing a hierarchical method to convert the extensive dataset into finite states, thereby enhancing its tractability. The discretisation procedure serves to simplify the interpretation of real-world instances, obviating the necessity for specialised expertise. For instance, wind speed is discretised into three distinct states namely low, medium, and high (as shown in Fig. 8), providing a lucid framework to interpret the findings. The correlation between various parameter states along with their conditional probability is computed using a complex BN algorithm as discussed in algorithm 2. The correlation output of wind speed with other weather parameters is shown in Fig. 8 and the corresponding conditional probability table is illustrated in Table V. This relationship, modeled using a BN approach, is further utilised to find the range of uncertain parameters affected by the variations in other considered parameters.

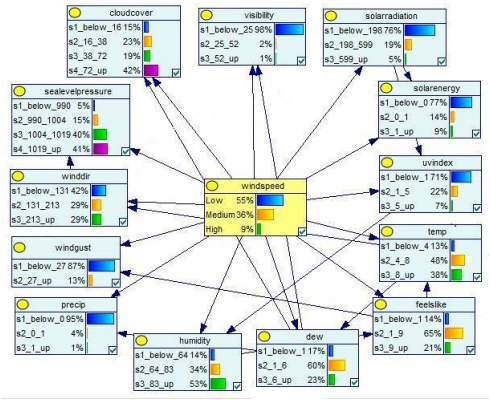

Fig. 8: Dependence of wind speed on weather parameters

After computing the range of values for solar radiation and wind speed, their respective power generation in each area with the help of Eq. (2) and (3) are then computed and are compared with their real time values. We have chosen one specific area A5 (i.e., Southshields) from Fig. 5 to show the detailed impact of uncertainty. On detection of an uncertain event in A5, the type of uncertainty is identified using Algorithm 2. Based on the algorithm, the area A5 suffers from data uncertainty at time $t1$, due to which its measured wind generation becomes zero, which was resolved by time $t4$ as shown in Fig. 9(a). Consequently, the local energy supply is disrupted, prompting the utilisation of battery storage to meet the load demand that can be seen from decreasing the SOC of the battery in Fig. 9(b). After $t2$, the battery is discharged to its maximum capacity, the area becomes dependent either on the grid or other neighbouring areas to buy energy to meet the load demand. There is an increase in grid purchase from $t2$ to $t3$ to meet the load demand of A5 (Fig. 9(c)), which corresponds to no excess renewable generation available from neighboring areas. From $t3$ to $t4$, the grid purchases became zero, showing that there is excess renewable energy generation in the neighbouring areas which is purchased by A5 to meet its load demand and charge the battery until the uncertainty is resolved at $t4$.

C. Uncertainty Mitigation

Upon uncertain event detection in phase B, our research employs a cooperative strategy to address the uncertainty in affected areas and minimise its impact on the overall operation of the DN. The battery storage of area A5 with uncertain event along with the battery storage of all neighbouring areas is leveraged in the cooperative strategy as detailed in Section III-C. In Fig. 10, SOC profiles of batteries from different areas selected using the algorithm 3 during uncertain situations are depicted. We compare two distinct scenarios where energy discharge from battery storage is managed equally and proportionately

TABLE V: Conditional Probability Table (CPT) for Windspeed and other weather parameters

windgust (%)	**windgust (<27)**	**windgust (>27)**	**windgust (>27)**
winddir (%)	**winddir (<131)**	**winddir (<131)**	**winddir (>325)**
sealevelpressure (%)	**sealevelpressure (<990)**	**sealevelpressure (<990)**	**sealevelpressure (<990)**
cloudcover (%)	**cloudcover (<16)**	**cloudcover (<16)**	**cloudcover (<16)**
windspeed (<11)	25%	2%	18%
windspeed (>11 & <21)	74%	75%	30%
windspeed (>21)	1%	23%	52%

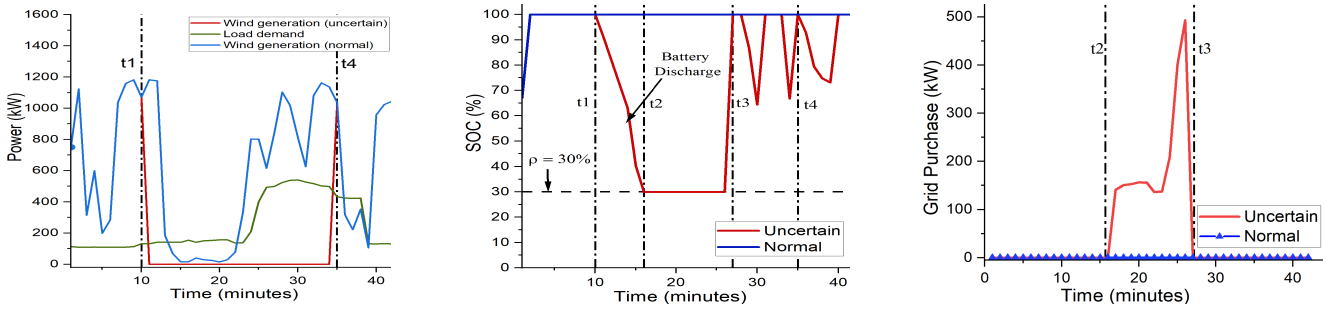

(a) (b) (c)

Fig. 9: Impact of uncertainty on (a) wind generation (b) SOC of the battery (c) power purchase from grid

among selected areas to meet the load demand of the affected area. Fig. 10(a) shows the outcome when an equal amount of energy is drawn from the battery storage across all selected areas. When energy discharge is uniform across all areas, the SOC trajectory shows fluctuations and fails to reach its maximum capacity, indicative of sub-optimal battery utilisation and potentially accelerated degradation. Fig. 10(b) showcases a strategic approach, distributing energy discharge in proportion to each area's capacity using the cooperative algorithm.

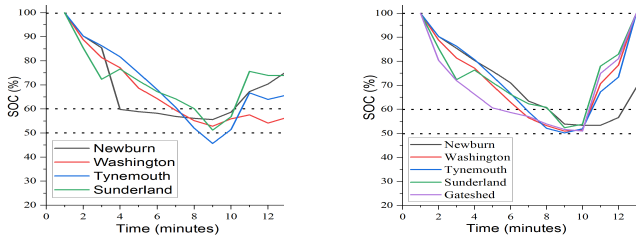

(a) (b)

Fig. 10: SOC of different areas using cooperative approach when energy is shared (a) equally (b) proportionally

Under the proportionate energy discharge strategy, there is a smooth trend in the battery's discharge and recharge cycles. This smoother operational pattern hints at reduced battery degradation, attributed to the balanced and optimised utilisation of energy resources across the network.

We further extend our analysis to compare the overall profit and carbon emissions during uncertainty using three different strategies: competitive, cooperative-equal sharing, and cooperative-proportionate sharing as shown in Fig. 11.

Fig. 11(a) illustrates the overall profit during the uncertain period. The results indicate that the competitive algorithm achieves 16.4% higher profit as compared to the cooperative-proportionate sharing method. This is because the competitive strategy prioritises maximising an individual area's profit. However, the higher profit comes at a significant environmental cost. Fig. 11(b) presents a comparison of carbon emissions among the three strategies. Fig. 11 demonstrates that the reduction in carbon emissions between the two methods ranges from 0% to 97% throughout the uncertain scenario considered, with an average reduction of 48.2% with the cooperative proportionate

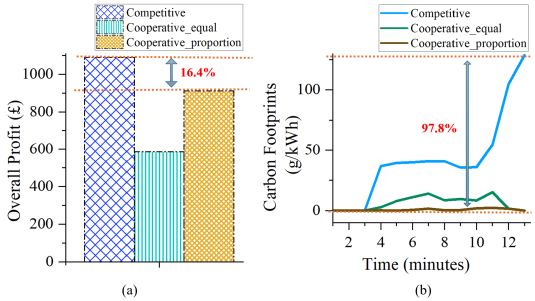

(a) (b)

Fig. 11: Comparison of different approaches under uncertainty for (a) overall profit (b) carbon footprints

sharing method as compared to the competitive approach. Overall, the competitive algorithm is used under normal conditions to maximise immediate profits without overburdening the batteries. In contrast, the cooperative-proportionate strategy is employed during uncertainties, leveraging the battery storage capacities of neighboring areas to support the affected area. This two-fold approach ensures both the economic benefits and environmental sustainability of the energy system, optimising resource utilisation during normal operations, and enhancing reliability during uncertain conditions.

V. Conclusion

The integration of DERs into DNs introduces various uncertainties, such as unpredictable renewable energy outputs, fluctuating consumer energy demands, and data or equipment faults. In this study, we implemented a two-fold strategy to manage the system under normal and uncertain conditions. During normal operations, a competitive algorithm maximises profit and ensures efficient market functioning, along with cutting down carbon footprints to one-fifth. In contrast, during uncertain conditions, a cooperative strategy with proportionate sharing stabilises the system by utilising the battery storage capacities of neighboring areas. Our results show that the cooperative-proportionate sharing method significantly reduces carbon emissions by a maximum of 97% compared to the competitive algorithm during uncertainty with an average reduction of 48.2%, while also ensuring a smoother SOC trend and reducing battery degradation. This approach balances economic

and environmental outcomes, enhancing the reliability and sustainability of renewable-integrated DNs.

In the future, the work will focus on modeling the uncertainty arising due to unpredictable consumer behavior at the planning stage and further reducing its impact on the DN operations.

ACKNOWLEDGEMENT

This work was supported by the Engineering and Physical Sciences Research Council [grant number EP/Y005376/1] – VPP-WARD Project, https://www.vppward.com. This work was partially supported by the Engineering and Physical Sciences Research Council - CHEDDAR Project [grant numbers EP/X040518/1, EP/Y037421/1].

REFERENCES

[1] H. Ritchie, P. Rosado, and M. Roser, "Breakdown of carbon dioxide, methane and nitrous oxide emissions by sector," *Our World in Data*, 2020, [Online] https://ourworldindata.org/emissions-by-sector.

[2] "Massive expansion of renewable power opens door to achieving global tripling goal set at cop28," https://www.iea.org/news/massive-expansion-of-renewable-power-opens-door-to-achieving-global-tripling-goal-set-at-cop28, accessed: 2024-05-24.

[3] G. Dhiman and N. S. Alghamdi, "Smose: Artificial intelligence-based smart city framework using multi-objective and iot approach for consumer electronics application," *IEEE Transactions on Consumer Electronics*, vol. 70, no. 1, pp. 3848–3855, 2024.

[4] F. Luo, Q. Bu, Z. Ye, Y. Yuan, L. Gao, and P. Lv, "Dynamic reconstruction strategy of distribution network based on uncertainty modeling and impact analysis of wind and photovoltaic power," *IEEE Access*, 2024.

[5] A. Jindal, A. K. Marnerides, A. Gouglidis, A. Mauthe, and D. Hutchison, "Communication standards for distributed renewable energy sources integration in future electricity distribution networks," in *ICASSP 2019-2019 IEEE International Conference on Acoustics, Speech and Signal Processing (ICASSP)*. IEEE, 2019, pp. 8390–8393.

[6] Q.-H. Wu, A. Bose, C. Singh, J. H. Chow, G. Mu, Y. Sun, Z. Liu, Z. Li, and Y. Liu, "Control and stability of large-scale power system with highly distributed renewable energy generation: Viewpoints from six aspects," *CSEE Journal of Power and Energy Systems*, vol. 9, no. 1, pp. 8–14, 2023.

[7] L. Chen, L. Liu, Y. Peng, W. Chen, H. Huang, T. Wu, and X. Xu, "Distribution network operational risk assessment and early warning considering multi-risk factors," *IET Generation, Transmission & Distribution*, vol. 14, no. 16, pp. 3139–3149, 2020.

[8] X. Wang, S. Li, and M. Iqbal, "Live power generation predictions via AI-driven resilient systems in smart microgrids," *IEEE Transactions on Consumer Electronics*, vol. 70, no. 1, pp. 3875–3884, 2024.

[9] A. Hentunen, J. Forsströmm, and V. Mukherjee, "Smart system of renewable energy storage based on integrated EVs and batteries to empower mobile, distributed and centralised energy storage in the distribution grid," *Horizon*, 2020.

[10] "Most of bangladesh left without power after national grid failure," https://edition.cnn.com/2022/10/04/asia/bangladesh-blackouts-power-grid-failure-intl/index.html/, accessed: 2024-05-24.

[11] P. S. Karagiannopoulos, N. M. Manousakis, and C. S. Psomopoulos, "3R practices focused on home appliances sector in terms of green consumerism: Principles, technical dimensions, and future challenges," *IEEE Transactions on Consumer Electronics*, vol. 70, no. 1, pp. 96–107, 2024.

[12] K. N. Hasan, R. Preece, and J. V. Milanović, "Existing approaches and trends in uncertainty modelling and probabilistic stability analysis of power systems with renewable generation," *Renewable and Sustainable Energy Reviews*, vol. 101, pp. 168–180, 2019.

[13] K. H. M. Azmi, N. A. M. Radzi, N. A. Azhar, F. S. Samidi, I. T. Zulkifli, and A. M. Zainal, "Active electric distribution network: applications, challenges, and opportunities," *IEEE Access*, vol. 10, pp. 134 655–134 689, 2022.

[14] X. Cao, J. Wang, and B. Zeng, "A chance constrained information-gap decision model for multi-period microgrid planning," *IEEE Transactions on Power Systems*, vol. 33, no. 3, pp. 2684–2695, 2017.

[15] Y. Jiang, C. Wan, C. Chen, M. Shahidehpour, and Y. Song, "A hybrid stochastic-interval operation strategy for multi-energy microgrids," *IEEE Transactions on Smart Grid*, vol. 11, no. 1, pp. 440–456, 2019.

[16] U. Oh, Y. Lee, J. Choi, and R. Karki, "Reliability evaluation of power system considering wind generators coordinated with multi-energy storage systems," *IET Generation, Transmission & Distribution*, vol. 14, no. 5, pp. 786–796, 2020.

[17] T. Ding, Q. Yang, Y. Yang, C. Li, Z. Bie, and F. Blaabjerg, "A data-driven stochastic reactive power optimization considering uncertainties in active distribution networks and decomposition method," *IEEE Transactions on Smart Grid*, vol. 9, no. 5, pp. 4994–5004, 2017.

[18] R. Khodabakhsh and S. Sirouspour, "Optimal control of energy storage in a microgrid by minimizing conditional value-at-risk," *IEEE Transactions on Sustainable Energy*, vol. 7, no. 3, pp. 1264–1273, 2016.

[19] T. Su, J. Zhao, Y. Pei, and F. Ding, "Probabilistic physics-informed graph convolutional network for active distribution system voltage prediction," *IEEE Transactions on Power Systems*, 2023.

[20] H. Wang, Z. Yan, M. Shahidehpour, Q. Zhou, and X. Xu, "Optimal energy storage allocation for mitigating the unbalance in active distribution network via uncertainty quantification," *IEEE Transactions on Sustainable Energy*, vol. 12, no. 1, pp. 303–313, 2021.

[21] Paredes, J. A. Aguado, and P. Rodríguez, "Uncertainty-aware trading of congestion and imbalance mitigation services for multi-dso local flexibility markets," *IEEE Transactions on Sustainable Energy*, vol. 14, no. 4, pp. 2133–2146, 2023.

[22] A. Garg, G. S. Aujla, and H. Sun, "Analyzing impact of data uncertainty in distributed energy resources using bayesian networks," in *2023 IEEE International Conference on Communications, Control, and Computing Technologies for Smart Grids (SmartGridComm)*. IEEE, 2023, pp. 1–6.

[23] "IEEE standard for interconnection and interoperability of distributed energy resources with associated electric power systems interfaces," *IEEE Std 1547-2018 (Revision of IEEE Std 1547-2003)*, pp. 1–138, 2018.

[24] N. M. Kumar, S. S. Chopra, A. A. Chand, R. M. Elavarasan, and G. Shafiullah, "Hybrid renewable energy microgrid for a residential community: A techno-economic and environmental perspective in the context of the SDG7," *Sustainability*, vol. 12, no. 10, p. 3944, 2020.

[25] A. Garg, G. S. Aujla, and H. Sun, "Techno-economic-environmental analysis for net-zero sustainable residential buildings," in *2023 IEEE PES Innovative Smart Grid Technologies Europe (ISGT EUROPE)*. IEEE, 2023, pp. 1–5.

[26] T. Ma and M. S. Javed, "Integrated sizing of hybrid pv-wind-battery system for remote island considering the saturation of each renewable energy resource," *Energy conversion and management*, vol. 182, pp. 178–190, 2019.

[27] R. J. J. Molu, S. R. D. Naoussi, P. Wira, W. F. Mbasso, S. T. Kenfack, B. K. Das, E. Ali, M. J. Alshareef, and S. S. Ghoneim, "Optimizing technical and economic aspects of off-grid hybrid renewable systems: A case study of manoka island, cameroon," *IEEE Access*, vol. 11, pp. 130 909–130 930, 2023.

[28] R. Deng, Z. Yang, F. Hou, M.-Y. Chow, and J. Chen, "Distributed real-time demand response in multiseller–multibuyer smart distribution grid," *IEEE Transactions on Power Systems*, vol. 30, no. 5, pp. 2364–2374, 2015.

[29] J. Contreras, M. Klusch, and J. B. Krawczyk, "Numerical solutions to nash-cournot equilibria in coupled constraint electricity markets," *IEEE Transactions on Power Systems*, vol. 19, no. 1, pp. 195–206, 2004.

[30] "Weather data," https://www.visualcrossing.com/weather/weather-data-services, accessed: 2023-05-03.

[31] "Energy prices," https://octopus.energy/octopus-smart-tariffs/, accessed: 2024-04-17.

[32] D. Dragone, L. Lambertini, and A. Palestini, "Static and dynamic best-response potential functions for the non-linear cournot game," *Optimization*, vol. 61, no. 11, pp. 1283–1293, 2012.